I J Radiol. 2026 March; 23(1): e167871 https://doi.org/10.5812/iranjradiol-167871

Published Online: 2026 May 17

Research Article

Differences in Ultrasound Characteristics Among Molecular Subtypes of Breast Cancer: A Retrospective Cross-Sectional Analysis

Mobina Abbasi [1,2], Mohammadreza Tahamtan [1,2], Nahid Sadighi [1,2], Saeed Mohammadzadeh [1,2], Peyman Kamali Hakim [3], Fatemeh Shakki Katouli [1,2], Maryam Aghasi [1,2], Fahimeh Zeinalkhani [1,2,*]

[1] Advanced Diagnostic and Interventional Radiology Research Center (ADIR), Tehran University of Medical Sciences, Tehran, Iran
[2] Department of Radiology, Tehran University of Medical Sciences, Imam Khomeini Hospital, Tehran, Iran
[3] Radiology Department, Iran University of Medical Sciences, Tehran, Iran

[*] ***Corresponding Author:*** Advanced Diagnostic and Interventional Radiology (ADIR) Tehran University of Medical Sciences Imam Khomeini Hospital Complex (IKHC), 2nd Floor, Tehran, Iran. Email: f_zeinalkhani@yahoo.com

Received: 16 November, 2025; **Revised:** 5 May, 2026; **Accepted:** 9 May, 2026

Abstract

Background: Breast cancer molecular subtyping is crucial for prognosis and treatment planning, prompting interest in noninvasive ultrasound-based approaches for identifying relevant correlations.

Objectives: Breast cancer, which is highly prevalent worldwide, comprises several molecular subtypes, including luminal A (LA), luminal B (LB), triple-negative (TN), and human epidermal growth factor receptor 2-positive (HER2+). These subtypes have distinct prognostic and therapeutic implications. However, differences in ultrasound features among these subtypes and their potential associations with molecular classification remain underexplored.

Patients and Methods: This retrospective cross-sectional study analyzed data from 140 women with primary invasive breast cancer treated at a referral hospital between April 2022 and March 2023. Standard ultrasound imaging and comprehensive clinicopathological data, including molecular subtypes identified by immunohistochemistry, were evaluated. Statistical analyses were performed using SPSS version 22 to assess correlations between ultrasound features and molecular subtypes.

Results: The mean age of the participants was 49.75 years, and the mean tumor size was 27.1 mm. LA was the most common subtype (48%), followed by LB (25%), TN (18%), and HER2+ (7%). Adjusted associations between ultrasound features and molecular subtypes showed a nonsignificant trend, particularly for calcification, tumor shape, and tumor location. The TN subtype had the highest calcification rate, followed by the LA subtype (adjusted P = 0.107). Irregular shapes were common across all subtypes, whereas variation in the frequencies of round and oval shapes suggested potential subtype-specific differences.

Conclusion: Certain ultrasound features showed nonsignificant trends across molecular subtypes; however, these findings do not currently support reliable differentiation among subtypes. Further research is needed to validate these preliminary results and potentially expand the diagnostic role of ultrasound in breast cancer subtyping.

Keywords: Correlation, Molecular Subtypes, Breast Cancer, Pathology, Morphology, Ultrasonography

1. Background

Breast cancer is the most common cancer worldwide and a leading cause of cancer-related mortality and morbidity (1, 2). Cancer incidence and mortality rates pose increasing challenges to healthcare systems, particularly in low- and middle-income countries (2). The clinical management of breast cancer has been transformed by the recognition that it is not a single disease but a group of molecularly distinct subtypes. These subtypes, categorized primarily by the expression of estrogen receptor (ER), progesterone receptor (PR), and human epidermal growth factor receptor 2 (HER2), are divided into four groups: triple-negative (TN), luminal A (LA), luminal B (LB), and HER2-positive (HER2+) (3, 4). Breast cancer molecular subgroups differ

How to Cite: Abbasi M, Tahamtan M, Sadighi N, Mohammadzadeh S, Kamali Hakim P, et al. Differences in Ultrasound Characteristics Among Molecular Subtypes of Breast Cancer: A Retrospective Cross-Sectional Analysis. I J Radiol. 2026;23(1):e167871. doi: https://doi.org/10.5812/iranjradiol-167871

in biology, treatment options, and prognosis. When endocrine therapy and chemotherapy are combined, the prognosis of high-stage LA breast cancer is generally more favorable than that of other subtypes, and this subtype responds well to treatment. In contrast, the LB subtype typically has a poorer prognosis than the LA subtype. For HER2+ tumors, the development and use of targeted therapy are crucial (5). TN breast cancer is a highly aggressive subtype with limited therapeutic options and a poor prognosis. Therefore, accurate differentiation among breast cancer molecular subtypes is valuable for clinical diagnosis, treatment planning, and prognostic evaluation (6).

Currently, the gold standard for determining molecular subtype is immunohistochemistry (IHC) analysis of tissue samples obtained through core needle biopsy or surgery. However, biopsy procedures, including core needle, vacuum-assisted, and stereotactic biopsy, are invasive and are associated with risks such as hemorrhage, patient discomfort, and inadequate sampling (3, 6).

2. Objectives

Breast ultrasonography is an effective diagnostic tool for evaluating clinical or radiological abnormalities; however, its ability to differentiate among molecular subtypes of breast cancer remains largely unexplored (7). This study aimed to investigate the correlation between pathological molecular subtypes of breast cancer and their morphologic features on ultrasonography.

3. Patients and Methods

3.1. Patient Selection

Data from 140 consecutive patients with primary invasive breast cancer who underwent surgery at a referral hospital from April 2022 to March 2023 were collected. The institutional review board of Tehran University of Medical Sciences approved this retrospective cross-sectional study and waived the requirement for informed consent. Patient data were anonymized. Comprehensive histopathological data, including molecular subtype, along with clinical and ultrasonographic features, were collected for analysis. After approval, patients with pathology-confirmed breast cancer were identified and included in the study. Patients who underwent ultrasonographic evaluation using the Breast Imaging Reporting and Data System (BI-RADS) lexicon before pathological assessment with immunohistochemistry-based molecular subtyping, both performed at our center, were included. The exclusion criteria were as follows: (1) insufficient ultrasound or pathological data, (2) a history of other malignancies, and (3) breast cancer after chemotherapy or radiotherapy. A flowchart of the study population is shown in Figure 1.

3.2. B-Mode Ultrasound

Ultrasound images were acquired using a Voluson E6 system (GE Healthcare, Milwaukee, IL, USA) equipped with a 10 - 16 MHz linear probe. Patients with breast cancer whose ultrasound examinations were performed during the 1-year period were included. The examinations were performed by two highly experienced radiologists, each with at least 5 years of specialized expertise in breast imaging. Sonographic features were primarily extracted from ultrasound reports. When reports lacked specific required details, the original images were retrieved from the picture archiving and communication system and re-evaluated to ensure complete data collection. Both radiologists were blinded to histopathological results and molecular subtypes.

Ultrasonographic features of breast masses were recorded, including tumor size, shape (oval, round, or irregular), location (retroareolar, central, upper outer quadrant [UOQ], upper inner quadrant [UIQ], lower outer quadrant [LOQ], or lower inner quadrant [LIQ]), margins (circumscribed, indistinct, angular, microlobulated, or spiculated), echo pattern (hypoechoic, complex, isoechoic, or heterogeneous), posterior acoustic features (enhancement, shadowing, or none), and the presence of calcification. Discrepancies or uncertainties regarding ultrasound features were resolved by discussion and consensus between the two radiologists.

Patients with malignant pathology results were included, and pathology results were recorded according to cellular and molecular type.

3.3. Pathology

Ultrasound examinations were performed before core needle biopsy in all included cases. Pathology results after core needle biopsy were used to determine molecular subtypes. ER, PR, and HER2 expression levels

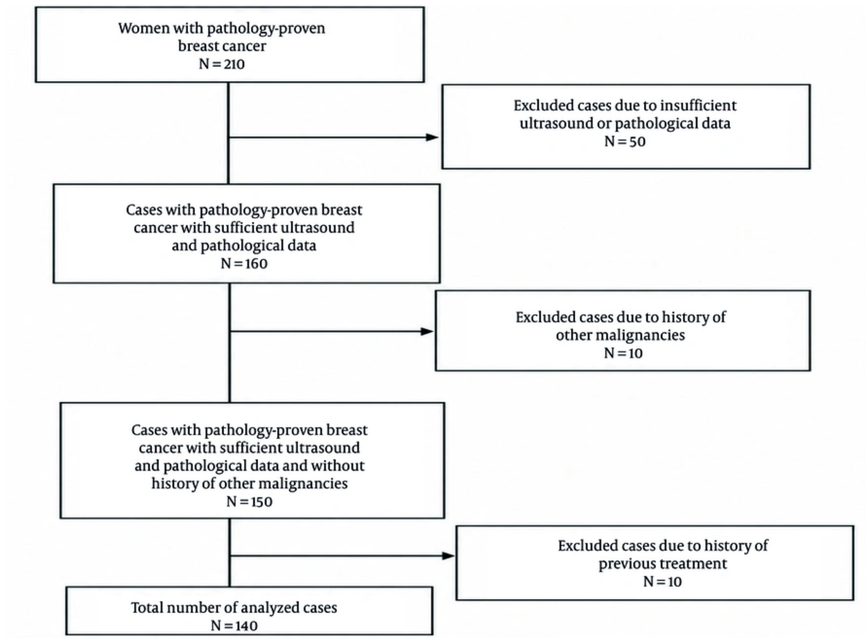

Figure 1. Flowchart of the study population

were measured using standard IHC staining. Nuclear staining of ≥ 1% and ≥ 20% indicated positive ER and PR expression, respectively. A 3+ cell membrane stain or fluorescence in situ hybridization analysis with a threshold ratio of ≥ 2.2 was used to identify HER2 positivity. The Ki-67 index cutoff value for distinguishing LA from LB subtypes was 14% (8).

Breast cancers were classified into four molecular subtypes based on ER, PR, HER2, and Ki-67 expression: (1) LA subtype (ER+, PR+, HER2–, Ki-67 < 14%); (2) LB subtype, further subdivided into the HER2– subtype (ER+, HER2–, and at least one of Ki-67 ≥ 14% or PR < 20%) and the HER2+ subtype (ER+, HER2+, any Ki-67 value, and any PR value); (3) HER2+ subtype (HER2+, ER–, PR–); and (4) TN subtype (ER–, PR–, HER2–), according to the St. Gallen consensus of 2013 (6).

3.4. Statistical Analysis

IBM SPSS Statistics version 22 (IBM Corp. Released 2013. IBM SPSS Statistics for Windows, Version 22.0. Armonk, NY: IBM Corp.) was used to analyze the data. There were no missing ultrasound or pathology data among the included patients, as all cases with insufficient information were excluded according to the study inclusion criteria. Quantitative results are expressed as mean ± standard deviation (SD), and qualitative variables are presented as percentages. Depending on whether the variable was quantitative or qualitative, the Kruskal-Wallis test or chi-square test was used to compare groups according to molecular subtype. Multiple testing correction was performed using the Benjamini-Hochberg false discovery rate method to control the expected proportion of false positives while maintaining adequate statistical power for this exploratory analysis across ultrasound features. A post-hoc power analysis was conducted for the primary statistical method, the chi-square test of independence, to justify the sample size. For a contingency table with degrees of freedom = 3, such as comparison of a binary ultrasound feature across four subtypes, an alpha level of 0.05 and a medium effect size (Cramer's V = 0.30), a sample size of 140 provides 91.2% power to detect a statistically significant association. A P-value of 0.05 was considered statistically significant.

4. Results

A total of 140 women participated in this study. The mean age at diagnosis was 49.75 ± 10.6 years (range, 26 -

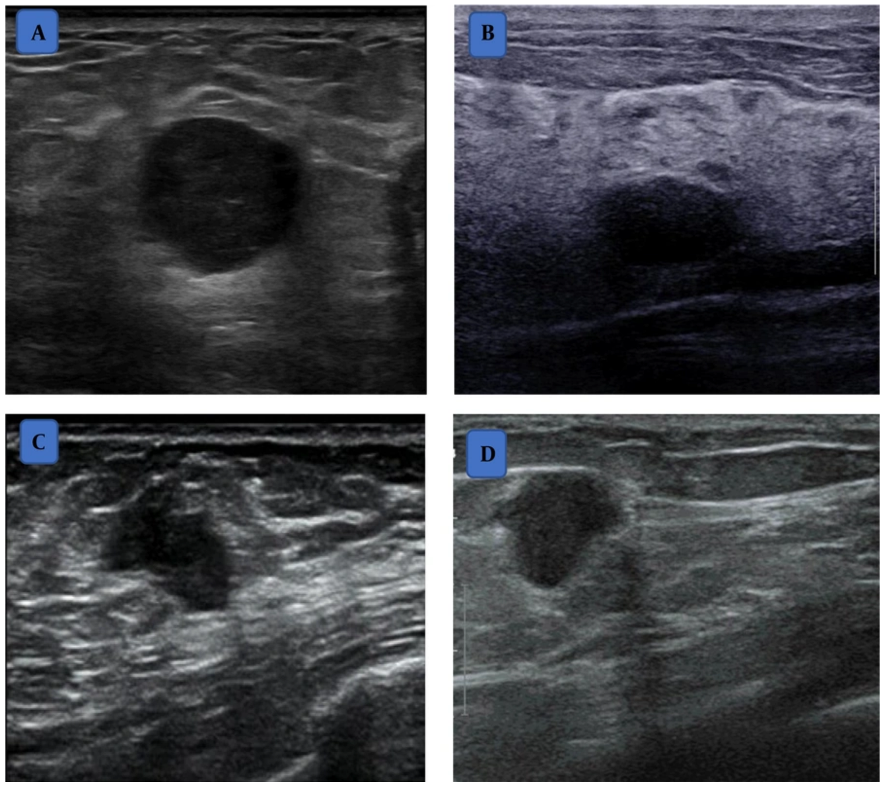

Figure 2. Ultrasound images of four malignant breast masses. A, A 38-year-old woman with a round shaped mass at the 10 o'clock position of the left breast, proven to be triple-negative invasive ductal carcinoma (IDC) on histopathological evaluation; B, A 40-year-old woman with an oval shaped mass at the 2 o'clock position of the left breast, proven to be luminal A IDC on histopathological evaluation; C, A 42-year-old woman with an irregular shaped mass at the 10 o'clock position of the right breast, proven to be HER2+ infiltrating ductal carcinoma on histopathological evaluation; D, A 44-year-old woman with an irregular shaped mass at the 3 o'clock position of the right breast, proven to be luminal B IDC on histopathological evaluation.

73 years). The most prevalent histologic subtypes were invasive ductal carcinoma (IDC) (90.7%, n = 127) and invasive lobular carcinoma (ILC) (5%, n = 7). Other histologic subtypes included medullary carcinoma (1.4%, n = 2), invasive mucinous carcinoma (1.4%, n = 2), mixed IDC and ILC (0.7%, n = 1), and mixed IDC and invasive micropapillary carcinoma (0.7%, n = 1). The mean tumor size on ultrasound was 27.1 ± 18.5 mm (range, 3 - 130 mm). No statistically significant correlation was observed between patient age or tumor size on ultrasound and molecular subtype (P = 0.9). The molecular subtype distribution was as follows: LA, 48% (n = 68); LB, 25% (n = 36); HER2+, 7% (n = 10); and TN, 18% (n = 26). Biomarker distribution was as follows: 74.3% were ER+, 67.9% were PR+, 29.3% were HER2+, and 80% showed high Ki-67 expression.

The TN subtype had the highest calcification rate (30.7%), followed by the LA subtype (29.4%). However, the correlation between calcification and molecular subtype was not significant (adjusted P = 0.107).

Regarding tumor shape on ultrasound, an irregular shape was the most prevalent pattern across all groups (LB: 30/36 [83.3%], LA: 53/68 [77.9%], HER2+: 8/10 [80.0%], and TN: 18/26 [69.2%]). A round shape was least common in the LB subtype (2/36 [5.6%]) and most common in the TN subtype (5/26 [19.2%]), whereas an oval shape showed a similar distribution across subtypes (11.1%-11.8%). These differences suggest possible subtype-specific morphologic patterns (Figure 2). However, the correlation between tumor shape and molecular subtype was not statistically significant (adjusted P = 0.107).

A statistically non-significant association was observed between molecular subtype and tumor location (adjusted P = 0.107). Most tumors were located

Table 1. Ultrasonographic Features According to Molecular Subtype of Breast Cancer [a]

Parameters	LB (n = 36)	LA (n = 68)	HER2+ (n = 10)	TN (n = 26)	Unadjusted P-value	Adjusted P-value
Tumor size (mm); mean (SD)	30.2 (25.2)	25.5 (14.7)	29.7 (21.5)	25.7 (13.9)	0.90	0.90
Calcification presence					0.029	0.107
Yes	7 (19.4) (6.5 - 32.4)	20 (29.4) (18.6 - 40.2)	2 (20.0) (0 - 44.8)	8 (30.7) (13.0 - 48.5)		
No	29 (80.6) (67.6 - 93.5)	48 (70.6) (59.8 - 81.4)	8 (80.0) (55.2 - 100)	18 (69.3) (51.5 - 87.0)		
Shape					0.038	0.107
Irregular	30 (83.3) (71.2 - 95.5)	53 (77.9) (68.1 - 87.8)	8 (80.0) (55.2 - 100)	18 (69.2) (51.5 - 87.0)		
Round	2 (5.6) (0 - 13.0)	7 (10.2) (3.1 - 68)	1 (10.0) (0 - 28.6)	5 (19.2) (4.1 - 34.4)		
Oval	4 (11.1) (0.8 - 21.4)	8 (11.8) (4.1 - 19.4)	1 (10.0) (0 - 28.6)	3 (11.6) (0 - 23.8)		
Margins					0.60	0.84
Microlobulated	5 (13.9) (2.6 - 25.2)	13 (19.1) (9.8 - 28.5)	1 (10.0) (0 - 28.6)	4 (15.3) (1.5 - 29.3)		
Spiculated	18 (50.0) (33.7 - 66.3)	33 (48.5) (36.7 - 60.4)	7 (70.0) (41.6 - 98.4)	7 (26.9) (9.9 - 44.0)		
Angular	3 (8.3) (0 - 17.4)	9 (13.2) (5.2 - 21.3)	1 (10.0) (0 - 28.6)	5 (19.2) (4.1 - 34.4)		
Indistinct	8 (22.2) (8.6 - 35.8)	11 (16.1) (7.4 - 24.9)	1 (10.0) (0 - 28.6)	8 (30.7) (13.0 - 48.5)		
Circumscribed	2 (5.6) (0 - 13.0)	2 (2.9) (0 - 7.0)	0 (0.0) (0 - 0)	2 (7.8) (0 - 17.9)		
Tumor location					0.046	0.107
UOQ	27 (75.0) (60.9 - 89.1)	44 (64.7) (53.3 - 76.1)	5 (50.0) (19.0 - 81.0)	15 (57.7) (38.7 - 76.7)		
UIQ	3 (8.3) (0 - 17.4)	8 (11.7) (4.1 - 19.4)	2 (20.0) (0 - 44.8)	5 (19.2) (4.1 - 34.4)		
LOQ	3 (8.3) (0 - 17.4)	4 (5.9) (0.3 - 11.5)	0 (0.0) (0 - 0)	2 (7.7) (0 - 17.9)		
LIQ	2 (5.6) (0 - 13.0)	4 (5.9) (0.3 - 11.5)	1 (10.0) (0 - 28.6)	0 (0.0) (0 - 0)		
Central	0 (0.0) (0 - 0)	3 (4.4) (0 - 9.3)	0 (0.0) (0 - 0)	1 (3.8) (0 - 11.2)		
Retroareolar	1 (2.8) (0 - 8.1)	5 (7.3) (1.1 - 13.6)	2 (20.0) (0 - 44.8)	3 (11.5) (0 - 23.8)		
Posterior acoustic features					0.30	0.525
Enhancement	2 (5.6)	7 (10.2) (3.1 - 17.5)	1 (10.0) (0 - 28.6)	0 (0.0) (0 - 0)		
Shadowing	22 (61.1)	39 (57.4) (45.6 - 69.1)	4 (40.0) (9.6 - 70.4)	12 (46.1) (27.0 - 65.3)		
None	12 (33.3)	22 (32.4) (21.2 - 43.5)	5 (50.0) (19.0 - 81.0)	14 (53.9) (34.7 - 73.0)		
Echogenicity					0.90	0.90
Hypoechoic	28 (77.8) (64.2 - 91.4)	52 (76.4) (66.4 - 86.6)	9 (90.0) (71.4 - 100)	21 (80.7) (65.6 - 95.9)		
Isoechoic	0 (0.0) (0 - 0)	1 (1.4) (0 - 4.3)	0 (0.0) (0 - 0)	0 (0.0) (0 - 0)		
Complex (complicated cyst)	0 (0.0) (0 - 0)	1 (1.4) (0 - 4.3)	0 (0.0) (0 - 0)	0 (0.0) (0 - 0)		
Heterogeneous	8 (22.2) (8.6 - 35.8)	14 (20.5) (11 - 30.2)	1 (10.0) (0 - 28.6)	5 (19.3) (4.1 - 34.4)		

Abbreviations: LB, luminal B; LA, luminal A; HER2+, human epidermal growth factor receptor 2-positive; TN, triple-negative; SD, standard deviation; CI, confidence interval; UOQ, upper outer quadrant; UIQ, upper inner quadrant; LOQ, lower outer quadrant; LIQ, lower inner quadrant.

[a] Values are expressed as No. (%) (95% CI).

in the UOQ across all groups, with frequencies ranging from 50.0% to 75.0%. The UIQ had the second-highest frequency, particularly in the HER2+ (20.0%) and TN (19.2%) groups. Tumors in the LOQ and LIQ were less common. UOQ location was most frequent in the LB subtype (75%) compared with other molecular subtypes, whereas this location had the lowest prevalence in the HER2+ subtype (50%). Central and retroareolar locations were the least common, although the retroareolar area showed notable frequencies in the HER2+ (20.0%) and TN (11.5%) groups.

Statistical analysis revealed no significant correlation between molecular subtype and acoustic enhancement, echogenicity, margins, or posterior acoustic features of the tumor. Detailed ultrasonographic characteristics of the included patients are summarized in Table 1.

Although unadjusted analyses showed statistically significant associations of calcification, tumor shape, and tumor location with molecular subtype, these associations were not significant after false discovery rate adjustment. Therefore, the observed differences represent numerical trends that should be interpreted cautiously and require confirmation in future studies.

5. Discussion

Identifying molecular characteristics specific to different subtypes of human breast cancer is crucial for informing clinical treatment options, understanding disease progression, and improving patient prognosis (5). Although pathological evaluation is standard practice for most breast cancers, ultrasonography can serve as an initial, accessible diagnostic tool and may provide clinicians with clues for differentiating molecular subtypes. The microscopic characteristics of breast cancer subtypes are distinct, and some studies suggest that these subtypes may also exhibit differentiating ultrasonographic features (9). Accordingly, the present study aimed to investigate ultrasonographic variations across different molecular subtypes. The main contribution of this study is its comprehensive comparative analysis of a broad panel of ultrasonographic features across all four major molecular subtypes within a single, well-defined regional cohort.

The mean age of the breast cancer patients in this study was 49.75 years. Khalaf et al. reported a mean age of 52 years among 160 patients, and Rashmi et al. also reported a mean age of 52 years, both of which are comparable to the mean age in our study (7, 10). Overall, the mean age of breast cancer patients at our center was comparable to that reported in other centers worldwide.

Our study indicated that the LA subtype usually appeared as a hypoechoic mass (76%) with posterior acoustic shadowing (57.4%) and irregular margins (78%). Although not statistically significant, shadowing occurred more frequently in the LA and LB groups than in the other groups. Khalaf et al. reported that the LA subtype generally presented as a mass with spiculated or angular margins and posterior acoustic shadowing (7). Moreover, Zhang et al. reported acoustic shadowing as a possible feature of the LA subgroup (11). These findings are consistent with our results, suggesting that posterior acoustic shadowing may be a characteristic feature of the LA subgroup. The LA subgroup is slow growing and is considered a low-grade tumor. Tumors exhibiting acoustic shadowing may reflect desmoplastic reactions, which are more common in low-grade tumors. This phenomenon occurs because the tumor reflects or attenuates sound more than the surrounding tissue (12).

We observed that the TN group had the highest frequency of round tumors among all subtypes. In addition, non-shadowing posterior features were most prevalent in the TN and HER2+ groups. Wojcinski et al. compared the ultrasonographic features of TN breast cancers with those of non-TN cancers and reported that TN cancers tend to have more round and oval shapes and more non-shadowing posterior features than non-TN cancers (13). However, posterior acoustic enhancement and lobulated or microlobulated margins, which were mentioned in the above study, were not more prevalent in our study than in the other subtypes. Non-shadowing posterior features can be attributed to the characteristic growth pattern of TN tumors, which often have a “pushing border” without an infiltrating margin. In addition, the high mitotic rate and increased cellularity, with minimal desmoplastic reaction observed pathologically in TN tumors, may appear as non-shadowing posterior features on ultrasound imaging (7, 13). In our study, the TN subtype showed the highest calcification rate (30.7%), followed by the LA subtype (29.4%). This finding contradicts the study by Khalaf et al., which identified calcification as a predictive factor for the HER2+ and LB subtypes. Further research is needed to explore this discrepancy (7).

In our study, the HER2+ subtype did not show statistically significant differences in any parameters compared with the other subtypes. Although some reports have indicated that posterior acoustic enhancement or no posterior change, calcification, and an abrupt mass boundary interface may be associated with the HER2+ subtype, we did not observe similar results in our study (7, 14, 15).

The LB subtype, which biologically lies between the LA and HER2 subtypes, showed characteristics intermediate between those observed in the LA and HER2 tumor subtypes. In our study, irregular margins were observed slightly more frequently in the LB subtype. Similar results were reported by Khalaf et al., who demonstrated that nodal metastasis and an irregular border were significantly associated with the LB subtype (7). A study by Zhang et al. suggested that the LB subtype is characterized by the absence of an echogenic halo and the presence of vascularity (11). Yang et al. noted that the lack of retraction phenomena and the presence of calcification were predictive factors for the LB subtype when using three-dimensional ultrasound; however, these findings do not align with our results (12).

Another parameter evaluated in this study was breast cancer location in the four breast quadrants. We observed a possible numerical trend in differences among molecular subtypes according to tumor location, which has not been assessed in previous studies. Typically, the most common breast cancer location is the UOQ. Consistent with this general trend, all subtypes in our study were more common in this location (16). UOQ location was more frequent in the LB and LA subtypes, whereas retroareolar location was more frequently observed in the HER2+ and TN subtypes than in the other subtypes. Rummel et al. reported that tumors located in the central region are associated with poorer outcomes; however, this relationship is not solely dependent on location but is influenced by larger tumor size. Tumors in the central region are more difficult to detect, leading to larger size at diagnosis and, consequently, a less favorable prognosis (17). Despite these differences, given the non-significant adjusted P-values, the findings should be interpreted with caution. In addition, the small number of cases within specific tumor location subgroups may limit the reliability of the analysis and raise the possibility that the observed association may be due to chance.

This study had several limitations. First, the analysis was based on breast tumors from a single center and was conducted retrospectively. Second, the small sample size may have limited the statistical significance of the collected data. Third, this study did not evaluate nodal involvement or color Doppler features, which may be associated with molecular subtypes. Fourth, this study was limited by the absence of a formal interobserver agreement assessment, as imaging evaluations were performed by consensus between two radiologists. Although this approach supported the validity of the reported results, it precluded quantitative analysis of inter-reader variability. Ultrasound is a simple, low-cost imaging modality with important diagnostic value in a wide range of clinical conditions, including breast cancer; however, it is operator dependent (18, 19). Future studies should include independent readings by multiple observers to better assess the reproducibility of ultrasound results in differentiating IHC subtypes. Fifth, although the overall cohort was adequately powered to detect associations of medium effect size, the small number of HER2+ cases limits the statistical reliability and generalizability of findings specific to this molecular subtype. Finally, this study was limited by its descriptive design and the small HER2+ subgroup (n = 10), which precluded reliable multivariate modeling because of wide confidence intervals and the complexity of multiple comparisons across four subtypes. Future studies with larger cohorts could develop predictive models for molecular subtyping based on ultrasound features.

In conclusion, potential associations and non-significant numerical trends were observed among the various molecular subtypes of breast cancer regarding the presence of calcifications, tumor location, and tumor shape on sonography. However, these findings are exploratory and preliminary, and further validation in larger multicenter studies is required. Pathological evaluation and molecular subtype determination are routinely performed in many centers; however, ultrasonography, as an initial diagnostic modality, may also provide useful clues regarding molecular subtype and offer clinicians additional information that can support more personalized diagnostic and treatment approaches.

Footnotes

AI Use Disclosure The authors declare that no generative AI tools were used in the creation of this article.

Authors' Contribution Study concept and design: S. Mohammadzadeh; Acquisition of data: F. Shakki Katouli; Analysis and interpretation of data: M. Abbasi; Drafting of the manuscript: S. Mohammadzadeh; Critical revision of the manuscript: F. Zeinalkhani; Statistical analysis: P. Kamali Hakim; Study supervision: N. Sadighi; Critical revision of manuscript: M. Aghasi.

Conflict of Interests Statement All authors declare that they have no known competing financial interests or personal relationships that could have appeared to influence the work reported in this paper.

Data Availability The dataset presented in the study is available on request from the corresponding author during submission or after publication.

Ethical Approval This study is approved under the ethical approval code of IR.TUMS.IKHC.REC.1401.040.

Funding/Support This research did not receive any specific grant from funding agencies in the public, commercial, or not-for-profit sectors.

References

1. Mohammadzadeh S, Mohebbi A, Moradi Z, Abdi A, Mohammadi A, Hakim PK, et al. Diagnostic performance of Kaiser score in the evaluation of breast cancer using MRI: A systematic review and meta-analysis. *European Journal of Radiology*. 2025;**186**. 112055. [PubMed ID: 40121897]. https://doi.org/10.1016/j.ejrad.2025.112055.
2. Sung H, Ferlay J, Siegel RL, Laversanne M, Soerjomataram I, Jemal A, et al. Global Cancer Statistics 2020: GLOBOCAN estimates of incidence and mortality worldwide for 36 cancers in 185 countries. *CA Cancer J Clin*. 2021;**71**(3):209-249.
3. Wang GS, Zhu H, Bi SJ. Pathological features and prognosis of different molecular subtypes of breast cancer. *Mol Med Rep*. 2012;**6**(4):779-782. [PubMed ID: 22797840]. https://doi.org/10.3892/mmr.2012.981.
4. Turkoz FP, Solak M, Petekkaya I, Keskin O, Kertmen N, Sarici F, et al. Association between common risk factors and molecular subtypes in breast cancer patients. *Breast*. 2013;**22**(3):344-350. [PubMed ID: 22981738]. https://doi.org/10.1016/j.breast.2012.08.005.
5. Orrantia-Borunda E, Orrantia-Borunda E, Anchondo-Nuñe P, Acuña-Aguilar LE, Gómez-Valles FO, Ramírez-Valdespino CA, et al. Subtypes of breast cancer. In: Mayrovitz HN, editor. *Breast Cancer*. Exon Publications; 2022.
6. Wu T, Li J, Wang D, Leng X, Zhang L, Li Z, et al. Identification of a correlation between the sonographic appearance and molecular subtype of invasive breast cancer: A review of 311 cases. *Clin Imaging*. 2019;**53**:179-185. [PubMed ID: 30415183]. https://doi.org/10.1016/j.clinimag.2018.10.020.
7. Khalaf LMR, Herdan RA. Role of ultrasound in predicting the molecular subtypes of invasive breast ductal carcinoma. *Egyptian Journal of Radiology and Nuclear Medicine*. 2020;**51**(1). 138. https://doi.org/10.1186/s43055-020-00240-z.
8. Kittaneh M, Montero AJ, Glück S. Molecular profiling for breast cancer: A comprehensive review. *Biomark Cancer*. 2013;**5**:61-70. [PubMed ID: 24250234]. [PubMed Central ID: PMC3825646]. https://doi.org/10.4137/bic.s9455.
9. Wu M, Ma J. Association between imaging characteristics and different molecular subtypes of breast cancer. *Academic Radiology*. 2016;**24**.
10. Rashmi S, Kamala S, Murthy SS, Kotha S, Rao YS, Chaudhary KV. Predicting the molecular subtype of breast cancer based on mammography and ultrasound findings. *Indian J Radiol Imaging*. 2018;**28**(3):354-361. [PubMed ID: 30319215]. [PubMed Central ID: PMC6176670]. https://doi.org/10.4103/ijri.ijri_78_18.
11. Zhang L, Li J, Xiao Y, Cui H, Du G, Wang Y, et al. Identifying ultrasound and clinical features of breast cancer molecular subtypes by ensemble decision. *Sci Rep*. 2015;**5**(1). 11085. [PubMed ID: 26046791]. [PubMed Central ID: PMC4457139]. https://doi.org/10.1038/srep11085.
12. Yang Q, Liu HY, Liu D, Song YQ. Ultrasonographic features of triple-negative breast cancer: A comparison with other breast cancer subtypes. *Asian Pac J Cancer Prev*. 2015;**16**(8):3229-3232. [PubMed ID: 25921124]. https://doi.org/10.7314/apjcp.2015.16.8.3229.
13. Wojcinski S, Soliman AA, Schmidt J, Makowski L, Degenhardt F, Hillemanns P. Sonographic features of triple-negative and non-triple-negative breast cancer. *J Ultrasound Med*. 2012;**31**(10):1531-1541. [PubMed ID: 23011616]. https://doi.org/10.7863/jum.2012.31.10.1531.
14. Eslami B, Omranipour R, Bayani L, Seifollahi A, Saberi A, Jahanbin B, et al. Comparison of Standard and Vacuum Specimen Mammography in the Detection of Margin Status in Conservative Surgery for Breast Cancer: a Cross-Sectional Diagnostic Study: Margin detection with specimen mammography. *Arch Breast Cancer*. 2024;**11**(1).
15. Liang X, Li Z, Zhang L, Wang D, Tian J. Application of contrast-enhanced ultrasound in the differential diagnosis of different molecular subtypes of breast cancer. *Ultrason Imaging*. 2020;**42**(6):261-270. [PubMed ID: 33019918]. https://doi.org/10.1177/0161734620959780.
16. Shah A, Haider G, Abro N, Hashmat S, Chandio S, Shaikh A, et al. Correlation between site and stage of breast cancer in women. *Cureus*. 2022;**14**(2). e22672. [PubMed ID: 35386160]. [PubMed Central ID: PMC8967127]. https://doi.org/10.7759/cureus.22672.
17. Rummel S, Hueman MT, Costantino N, Shriver CD, Ellsworth RE. Tumour location within the breast: Does tumour site have prognostic ability? *Ecancermedicalscience*. 2015;**9**:552. [PubMed ID: 26284116]. [PubMed Central ID: PMC4531129]. https://doi.org/10.3332/ecancer.2015.552.
18. Ebrahimian S, Akbari A, Soleimani Varaki S, Amirhosseini S, Akbari ME, Ashoftebargi S. Accuracy of MRI versus ultrasound/mammography in detecting axillary lymph node involvement in patients with breast cancer. *Int J Cancer Manag*. 2025;**18**(1). e162212. https://doi.org/10.5812/ijcm-162212.
19. Heidarzadeh H, Nazeri N, Forghani MN, Bakhtiari E, Alamdaran SA. Can highly specific ultrasound criteria obviate the need for sentinel lymph node biopsy in breast cancer patients with axillary lymph node metastasis? *I J Radiol*. 2024;**21**(1). e139030. https://doi.org/10.5812/ijradiol-139030.